

# Diagnosing and Modeling Common-Mode Radiation from Printed Circuit Boards with Attached Cables

J. L. Drewniak, Fei Sha, T. P. Van Doren, T. H. Hubing  
Department of Electrical Engineering  
Electromagnetic Compatibility Laboratory  
University of Missouri–Rolla  
Rolla, Missouri, 65401

J. Shaw  
Allison Transmission  
A Division of General Motors  
Indianapolis, IN 46206

## Abstract

A procedure for diagnosing and modeling radiation from printed circuit boards with attached cables is presented through a case study of a production model electronic control unit. Procedures for determining EMI antennas, IC sources, and mechanisms by which noise is coupled from the IC source to the antenna are suggested.

## 1 Introduction

As digital data rates and clock speeds continue to increase, with an accompanying increase in EMI problems, the need for characterizing, modeling, and anticipating EMI grows. A significant majority of EMI problems continues to be radiation from cables attached to the PCB, most often referred to as common-mode (CM) radiation. A typical EMI problem can be broadly broken into three components, the EMI antenna(s), specific IC source, and the mechanism or path by which energy is coupled from the IC to the antenna. The energy from the IC source might be an intended signal or clock, or may be an artifact of the IC's operation such as RF noise produced on the DC power bus by a switching device. In the case of CM radiation from cables, the antenna is comprised of two conductors of sufficient total electrical extent to form a radiator, one portion of which is a conductor(s) in the attached cable. Usually the EMI antenna is comprised of conductors that extend well beyond signal conductors. A potential difference between the two conductors drives this antenna. These types of EMI antennas are the focus of the present study and are referred to herein as "dipole-type" antennas. Though often a time-consuming and tedious task, the antennas can usually be identified. Likewise, the IC source driving the noise process can typically be determined through the process of enabling and disabling selective portions of the circuit, and well-thought engineering guesses. Identifying the mechanism or path by which energy is coupled from the IC source to the antenna is considerably more complex than determining the source or antenna. The coupling path is typically a function of layout features of the design.

A better knowledge of the three aspects of an EMI problem, IC source, antenna, and coupling mechanism, is required in order to diagnose problems rapidly. A more complete understanding of these fundamental aspects, and relating them to layout and design features of PCBs is

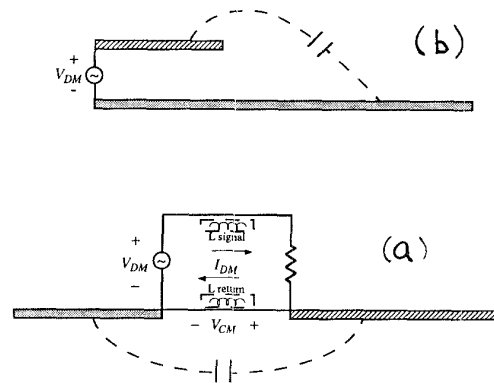


Figure 1: Wire circuit examples illustrating the physics of the a) current, and b) voltage driven mechanisms.

also required in order to anticipate and model EMI. At the prototype stage, only one of these aspects might be changeable, and a better knowledge of the problem, and development of adequate models can lead to relevant design changes.

## 2 Mechanisms of CM Radiation

Two fundamental mechanisms of CM radiation from PCBs with attached cables have previously been demonstrated [1], and are briefly summarized here [1]. The source mechanisms have been denoted *voltage-* and *current-driven* to distinguish the quantity that provides the driving mechanism of the CM current on the attached cable. A wire circuit example that illustrates the physics of the current-driven mechanism is shown in Figure 1 (a). If the loop inductance is decomposed into partial inductances for the upper and lower conductors [2], (assuming negligibly small partial inductance of the vertical branches) the large current through the partial inductance of the lower conductor results in a voltage drop. This voltage drop provides a source that can drive CM current on the extended lower conductor as shown. Thus the *current-driven* mechanism is directly related to the inherent finite impedance in ground (signal return) structures, or impedances associated with discontinuities in the ground structure. A wire circuit example illustrating the voltage driven mechanism is shown in Figure 1 (b). In this case the differential-mode

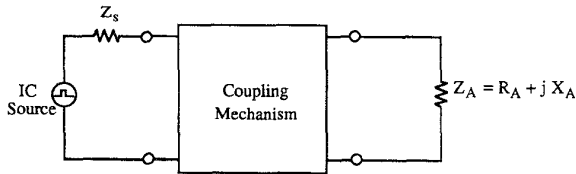


Figure 2: Schematic representation of components of an EMI problem: IC source, coupling mechanism, and antenna.

voltage provides the driving source that results in CM current. The extension of the return conductor beyond that of the signal conductor results in additional capacitance between the two conductors and an alternate current path. This alternate current path then results in CM current and CM radiation.

The previously described current- and voltage-driven mechanism concepts are being employed to develop techniques for diagnosing and anticipating EMI, in PCB designs. While these two mechanisms distinguish between the quantity voltage or current that results in the potential difference between two antenna conductors, the concepts are not in themselves complete. In particular, they do not adequately depict the mechanisms or paths through which current or voltage is coupled from specific IC sources or noise artifacts to antennas. Several coupling mechanisms are demonstrated experimentally and modeled for the production ECU of this study.

The current approach in developing diagnostic techniques and models assumes negligible interaction between antennas and coupling paths. While in the most general case this is not quite correct, in many EMI problems one particular radiator will dominate [3]. A general circuit diagram of the EMI radiator, which includes the three components indicated previously, the IC source, coupling mechanism, and antenna is shown in Figure 2. The coupling mechanism will include parasitic capacitances, inductances, and associated loss,  $Z_s$  is the source impedance, and  $Z_A$  is the antenna impedance for "dipole-type" radiators being considered. The coupling network will typically have one or more resonances in its transfer function, as will the antenna. Resonances of the coupling network and antenna that coincide can lead to significant EMI. Typically, two such complete radiators will not have peaks in the response over identical frequency ranges, or one will dominate. Thus, at this stage of development, mutual interactions between coupling mechanisms or EMI antennas are neglected.

A diagnostic technique for identifying CM radiation from cables attached to PCBs is being developed employing the ideas of two fundamental mechanisms, current- and voltage-driven, and the three components of an EMI radiator, IC source, coupling mechanism, and antenna. In the experimental procedures, the CM current on the attached cable is measured. The diagnostic and modeling procedure is conceptually a five step process: 1) identifying specific antenna conductors in the cable bundle; 2) identifying potential antenna parts on the PCB design or chassis; 3) identifying the IC source between two antenna conductors; 4) determining coupling paths; and, 5)

equivalent circuit modeling of the radiation process. The technique is presently not as simple as proceeding through these steps in a "cookbook" fashion. However, conceptually viewing the approach to an EMI problem within this framework can expedite the diagnosis and solution process.

First, the antenna conductors in the cable bundle are identified. A minimum power cable is employed to determine if the power or grounds in the cable bundle are significant parts of a radiator. Decoupling the power to ground can distinguish which conductor is the antenna part. Then, crude "voltage" probing at the connector pins with a spectrum analyzer and semi-rigid coaxial cable probe with an extended center conductor can indicate which remaining pins might have significant noise voltage relative to the ground. Of particular interest are those frequency ranges for which significant CM current on the cable bundle is measured. Then probing the connector pins with a long wire to function as a second antenna part can indicate which conductors in the cable bundle are primary candidates for an antenna piece in the cable bundle.

The second step is to identify other antenna pieces on the PCB, chassis, or cable imbalances that are being driven against a conductor in the cable bundle. In any PCB design there are typically only a few conductors of sufficient electrical extent that can be driven effectively against a conductor in the cable bundle to result in significant EMI. However, for signals at the full logic voltage that might be carried through a short flexible cable from one part of the design to another, the length of the conductor may be only a few short inches, but can result in significant EMI. Conductors at the PCB level that might form second antenna pieces include significant metal structures on the PCB such as inadequately grounded heatsinks, floating conductors, entire ground and power planes, flexible cables connecting two PCBs or parts of the design, or a PCB module plugged into a backplane, among others. Other conductors that can form second antenna pieces might be a conducting chassis, or imbalances in the cable. A long wire, e.g., 1 m, can be employed as a probe to enhance the radiation of potential antenna candidates. While this type of probing can couple sources to an artificially created antenna, these can usually be identified from an increase in the measured CM current at frequencies that were previously not significant. Probing with  $\vec{H}$ -field probes can also indicate conductors at the PCB level that are carrying relatively high currents. By qualitatively matching the probed spectrum to the measured CM-current spectrum, potential antenna pieces can also be identified.

The IC sources that might couple to the antennas can be identified, once the two portions of a "dipole-type" antenna are known. The specific IC source that couples to an antenna is often, but not always, located between the two antenna conductors. Typically, either clocks or data signals are coupled to antennas. These distinct sources can be distinguished from the measured CM-current spectrum. Radiation resulting from a clock line coupling to antenna structures is expected to have peaks at the clock harmonics, but little signal level in between, since the Fourier transform of a periodic signal has a discrete spectrum. This is illustrated in Figure 3 (a). However, data lines

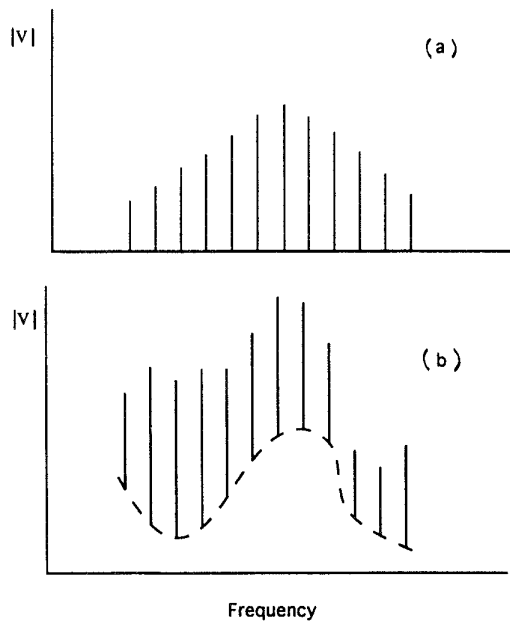


Figure 3: Radiation spectra from a) a purely periodic signal such as a clock, and, b) from a pseudo-random data signal initiated by the clock.

are switched at the clock frequency in a pseudo-random fashion that “fills” in these intermediate frequencies [4]. The result is an envelope with spectra corresponding to the clock harmonics superimposed as shown in Figure 3 (b). Selectively disabling clocks and data drivers usually indicates the specific IC source.

In general the most difficult task in diagnosing an EMI problem is determining the coupling path once the IC source and antenna have been identified. The coupling path will be comprised of parasitic capacitances and inductances that result from layout features. For example digital data lines running proximally to a large heatsink may capacitively couple current to the heatsink. This noise current returning to its source will result in a voltage drop from the heatsink conductor to the PCB ground if the heatsink is inadequately grounded because of the finite impedance (associated with inductance) of the ground connection. The ground in the cable bundle will be well connected to the PCB ground. Then an RF potential difference has been created between the heatsink and ground conductor in the cable bundle that results in EMI. While the effective source for this antenna configuration is located near one end, significant EMI can result at resonance frequencies of the antenna or equivalent coupling network. In this case, two conductors that are DC connected are driven against each other by a voltage developed as a result of a current through a finite impedance ground segment, and is referred to as a current-driven mechanism. This is just one example of many possibilities in a complex PCB design. However, the concepts of voltage-driven and current-driven effective sources are exploited to identify coupling paths in complex designs.

Finally, equivalent circuit diagrams that include the IC source, coupling mechanism, and antenna are constructed for the EMI problem. Equivalent circuit models can lead

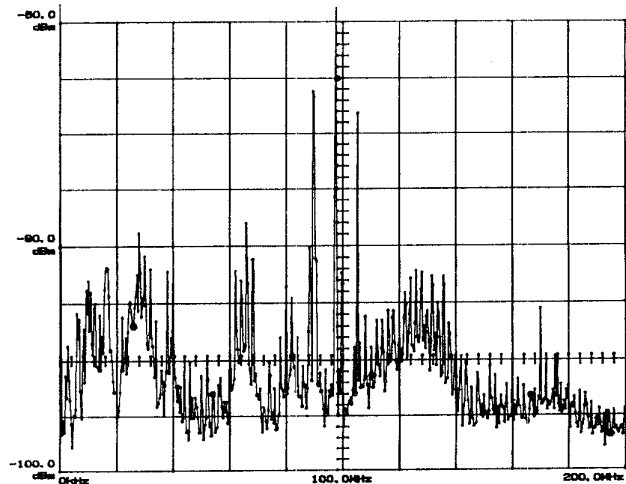


Figure 4: CM current on the attached cable bundle for ECU#1. 100 MHz center frequency, 20 MHz/div, -60 to -100 dB, 5 dB/div, 120 kHz RBW.

to a better understanding of the problem, as well as indicate potential EMI solutions that are not readily obvious. Typical changes in each of these aspects to reduce EMI include filtering clock or data signals (IC source), layout changes (coupling mechanism), and loading or filtering the antenna with ferrites and decoupling.

### 3 A Case Study

The previously described concepts and methods were applied to investigate EMI from a production electronic control unit (ECU). The CM-current measured on the attached cable bundle for the first generation ECU#1 of this study is shown in Figure 4. The measurements were conducted in an open room and significant ambients in the range of 95 – 105 MHz occur. Significant CM current in the frequency band 10 – 200 MHz is measured. The ECU design is a two PCB unit, with the boards separated by a 1.6” heatsink. A schematic representation of the design features pertinent to radiated emissions from the unit is shown in Figure 5. The unit was in a conducting (aluminum) enclosure with a 64-pin plastic shell connector that comprises the majority of one side of the ECU. Each PCB was a four layer board, with the upper board containing most of the logic and a logic ASIC, and the lower board the drivers for the outputs including an I/O ASIC. The upper and lower boards are designated the logic and power boards, respectively. The power and logic boards are connected by two 24 pin unshielded communications buses, only one of which is shown in Figure 5. Three grounds are designated in Figure 5, one each for the logic and power board, and an EMI ground that resides on the power board, but is connected to the power board ground through an RC filter. Most, but not all, I/O lines were decoupled to the EMI ground. The EMI ground was connected to the chassis through a conducting stud bonded to the heatsink. This connection was approximately 2” in from the connector as indicated by  $L_{EMI}$  in

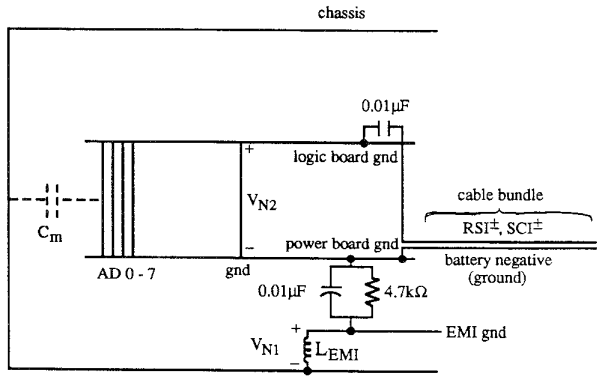


Figure 5: Schematic representation of the reduced ECU model relating sources and antennas to the physical geometry and circuit layout. The capacitance  $C_m$  and inductance  $L_{EMI}$  are parasitics.

Figure 5.

First a minimum cable bundle was constructed with lines only for powering the ECU. The resulting measured CM current was significant only in the range of 10 – 40 MHz, indicating that the antenna piece in the cable bundle was either power or ground. Subsequent measurements indicated that the antenna part was the ground conductor. The most likely candidate for the other part of the antenna was the aluminum chassis. Adding electrical length and loading to the chassis by touching it affected the measured CM current supporting this conjecture. The working assumption in pursuing the IC source was that the “dipole-type” antenna was the ground conductor in the cable bundle being driven against the chassis. These two conductors are connected by an RC filter as shown in Figure 5. The broadband nature of the measured CM-current spectra shown in Figure 4 in the range of 10 – 40 MHz indicates that the best candidates for the IC source are data drivers. The ECU was then removed from the chassis and the measured CM current increased by greater than 50 dB below 60 MHz. Probing with a long wire to provide a second antenna part indicated that the other part of the antenna with the ECU out of the case was data lines indicated in Figure 5 as AD0-7. Probing with an  $\vec{H}$ -field probe indicated high currents on these data lines in this frequency range as well. The proximity of the data lines to the chassis suggested that they might be capacitively coupling energy to the chassis as indicated in Figure 5 by the dashed element  $C_m$ . Tracing the return noise current path from the chassis back to the IC driving these data lines on the logic board showed that the connection of the chassis to the EMI ground was through very narrow traces. These narrow traces resulted in a significant impedance, indicated in Figure 5 by  $L_{EMI}$ , between the EMI ground and the chassis. The return noise current through this high RF impedance  $j\omega L_{EMI}$ , resulted in a potential difference  $V_{N1}$ , between the chassis and the EMI ground. The EMI ground was connected to the ground in the cable through a low RF impedance (0.01  $\mu F$  capacitor), and EMI in the frequency range 10 – 40 MHz resulted from the noise source  $V_{N1}$  driving the ground in the cable against the chassis. This coupling path is an

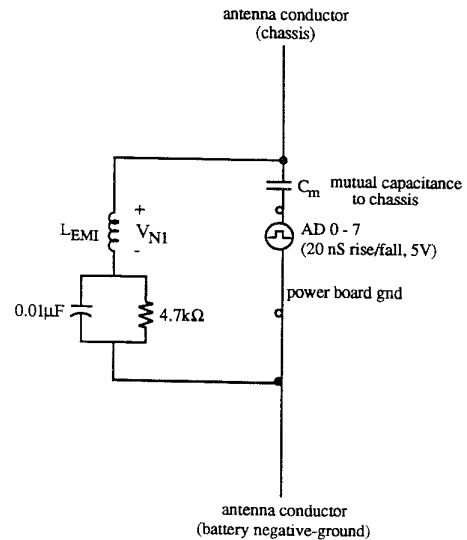


Figure 6: Equivalent circuit model for the EMI process in the 10 – 40 MHz frequency range for ECU#1.

example of a current-driven mechanism.

The equivalent circuit diagram shown in Figure 6 was constructed for this EMI process. An equivalent circuit for the data signals is not shown. The high impedance of the mutual capacitance from the AD0-7 data lines to the chassis relative to any loading on the order of a few hundred ohms with a ferrite sleeve indicates that loading would have little effect, and measurements supported this. Possible solutions in this case were to reduce the mutual capacitance  $C_m$  by employing a flexible cable with a planar ground, and/or reduce the impedance of the EMI ground to chassis connection. Design and manufacturing constraints precluded the use of a flexible cable with a planar ground, but the EMI ground was significantly modified to achieve a lower impedance connection between the EMI ground and chassis. The EMI ground and chassis connection for ECU#1 was modified with copper tape, and the measured CM current in the 10 – 40 MHz frequency range was reduced by 10 – 15 dB over the band. Radiated measurements in a stirred-mode chamber corroborated the improvement.

The schematic representation of the ECU shown in Figure 5 from which equivalent circuit models were developed also indicates that decoupling the I/O lines at the connector would not be particularly effective as a result of the high-impedance connection of the EMI ground to the chassis. Further investigations detailed below determining other antennas in the cable bundle that were driven against the chassis showed no improvement upon decoupling these antennas. However, when the EMI ground impedance was reduced, decoupling the I/O lines in the cable was effective.

A next generation ECU was produced that included an improved EMI ground to chassis connection. There were also significant changes in the logic board design as a result of a new logic ASIC. The CM-current measured on ECU#2 is shown in Figure 7. Significant improvements were obtained in the 10 – 40 MHz frequency range.

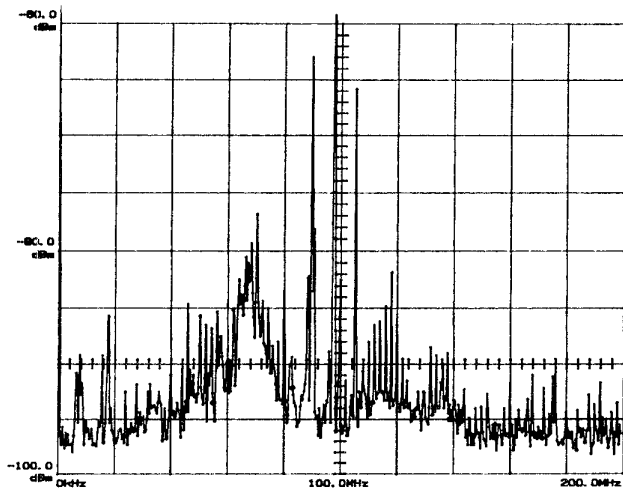


Figure 7: CM-current measurements on the cable of ECU#2. 100 MHz center frequency, 20 MHz/div, -60 to -100 dB, 5 dB/div, 120 kHz RBW.

However, the remaining portion of the measured spectrum indicates the same problem bands 60–90 MHz and 100–120 MHz as ECU#1. One of the antennas in the cable bundle that was associated with both of these bands was determined with ECU#1 to be communications lines denoted RSI<sup>±</sup> and SCI<sup>±</sup>, in Figure 5. These antennas were determined by “voltage” probing at the connector, and probing with a long wire for a second antenna part at each individual I/O pin with only minimum other connections to the ECU for power. The other part of the antenna against which the communications lines are driven is the chassis (and possibly the extended ground at the cable load end). Decoupling the RSI<sup>±</sup> and SCI<sup>±</sup> lines to the EMI ground after the copper tape modifications to the EMI ground of ECU#1 reduced the measured CM-current by greater than 10 dB in the 60–90 MHz. Effectively, the antenna had been shorted at the terminals at which the effective noise source appeared, i.e., the connector. However, prior to production of the next generation ECU#2, the specific IC source, and coupling mechanism of this IC source to the RSI<sup>±</sup> and SCI<sup>±</sup> antennas were unknown.

Further investigations on ECU#2 focussed on determining the specific IC source, and the coupling mechanism to the previously identified antenna. The 2, 4, and 8 MHz clocks were selectively disabled to determine that the primary noise source was being clocked at 2 MHz. The broadband nature of the measured CM-current indicated that the most likely candidates for the IC source were associated with data signals. All of the system clocks had rise times on the order of 2–30 ns. All clocks were filtered to slow the rise time to approximately 25–40 ns. However, filtering the clocks had no effect on the measured cable CM-current supporting the assertion that the associated source was driving data lines. Reductions in the CM-current were obtained, however, when the data lines AD0-7 lines between the logic and power boards were filtered at the IC device to slow the rise time.

After determining the IC source and the antenna, the coupling mechanism between these components was in-

vestigated. A noise voltage (relative to the power board ground) that appeared at the connector pins of the RSI<sup>±</sup> and SCI<sup>±</sup> I/O lines was the effective location of the driving source for the antenna. The antenna was the RSI<sup>±</sup> and SCI<sup>±</sup> lines being driven against the chassis. The RSI<sup>±</sup> and SCI<sup>±</sup> lines were traced on the layout and circuit diagrams from the connector to the device driving these lines. These lines were not decoupled at the connector, and went immediately from the power board to the logic board via a flexible cable (shown only with a single line in Figure 5). The lines then were decoupled to the logic board ground. Thus, any potential difference between the logic board ground, and the power board ground, would drive the RSI<sup>±</sup> and SCI<sup>±</sup> lines against the chassis. Recall that the impedance in the EMI to chassis connection denoted by  $L_{EMI}$  in Figure 5 had been reduced in ECU#2. The IC source was identified as the logic ASIC (on the logic board) driving the AD0-7 lines, which terminated at the I/O ASIC on the power board. A significant impedance in the path of these signals returning from the power board ground to the logic board ground results in a potential difference between the grounds of the two boards. The signal returns for the AD0-7 lines in the 24 pin flexible cable were relatively remote from the data lines. The AD0-7 were Lines 17-24, and the signal returns were Lines 3, 13, and 14. The large loop area of the signal return path resulted in a finite impedance associated with the partial inductance between the logic board ground and the power board ground. A potential difference between these grounds, denoted  $V_{N3}$  in Figure 5, then resulted from the return current from the AD0-7 signals. In the initial prototype ECU#2, the ground connections to the logic board for the signal returns of AD0-7 were inadvertently omitted as a result of layout artwork. The signal return for AD0-7 was then through the other flexible cable (carrying the RSI<sup>±</sup> and SCI<sup>±</sup> signals), further increasing  $L_3$  (see Figure 8). The measured data in Figure 7 was with this original configuration.

The equivalent circuit model shown in Figure 8 was developed for the source coupling mechanism to the antenna. The dashed lines in the model indicate potential solutions for minimizing EMI associated with this antenna, source, and coupling mechanism. These solutions were also employed to test the validity of the model. The inductances  $L_{EMI}$  and  $L_3$  denote the parasitic inductance associated with the finite impedance connection of the EMI ground to the chassis, and the partial inductance of the AD0-7 signal return path between the power and logic boards. The signal return current through  $L_3$  results in the potential difference  $V_2$  that drives the antenna. One solution is to “short” the antenna at its effective terminals by decoupling the RSI<sup>±</sup> and SCI<sup>±</sup> at the connector. Using 0.001  $\mu F$ , the resulting CM-current on the cable was reduced by approximately 10 dB in the frequency range of 60–90 MHz. However, this does not eliminate the coupling path. The coupling between the IC source and antenna can be reduced by lowering the impedance of the signal return path (reducing  $L_3$ ), or by RF shorting the antenna with a connection of the logic ground to the chassis through a 0.01  $\mu F$  capacitor. A connection to the chassis was available through several screws that went through the center of the design to mount the ECU in the chas-

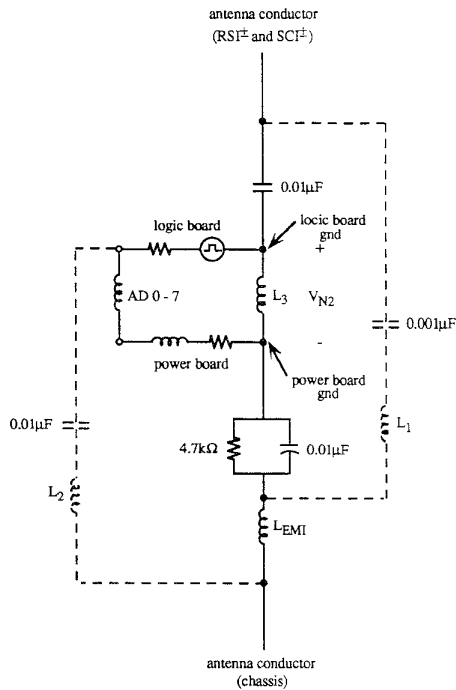


Figure 8: Equivalent circuit model for the EMI process in the 60 – 90 MHz frequency range.

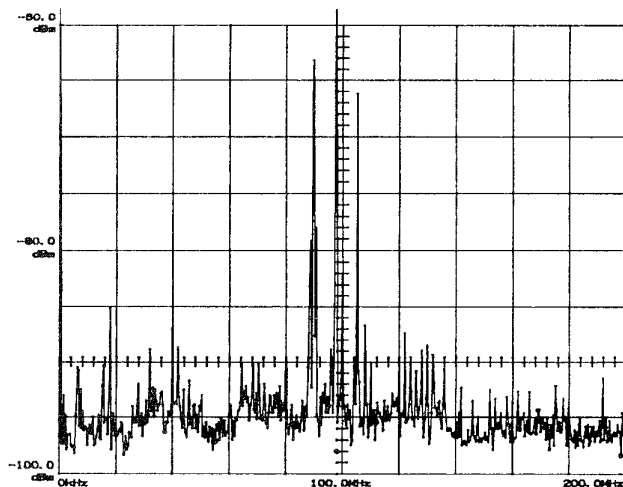


Figure 9: CM current measured on the cable of ECU#2 with the logic board ground connected to two chassis screws through 0.01 μF. 100 MHz center frequency, 20 MHz/div, -60 to -100 dB, 5 dB/div, 120 kHz RBW.

sis. A low-impedance connection from the logic board ground was made to two of these screws. The CM current measured on the cable with the logic ground connected through a 0.01 μF capacitor to the chassis is shown in Figure 9. There is a 10 – 15 dB reduction in the measured CM current on the cable at 60 – 90 MHz. A ground connection from the flexible cable carrying the AD0-7 signals to the logic ground was also made for these data. Measurements indicated that half the reduction came as a result of this connection.

## 4 Conclusion

Two previously demonstrated fundamental mechanisms have been employed in this study to develop a framework for systematically determining the IC source, antennas, and coupling mechanisms that comprise a typical EMI problem. While the method does not necessarily lead to the solution of any EMI problem with the application of a few “cookbook” steps, it does present a framework within which to work.

Equivalent circuit models were developed for the EMI problems associated with the production ECU studied. These models lent insight into the EMI problem and provided direction for solutions. However, while the circuit models included elements for the essential parasitics that coupled the IC source to the antenna, the values of these elements were undetermined. Further, no equivalent circuit models were developed for the known antennas. In order to estimate emissions with engineering accuracy employing a full-wave numerical electromagnetics code for modeling the gross antenna features, an equivalent noise source is required. Values for the parasitic elements of the coupling mechanism are necessary to obtain an equivalent noise source to employ with numerical codes. Finally, the coupling mechanisms are typically associated with layout features of the design. One particular design was investigated in this study and two specific coupling mechanisms reported. However, while the current- and voltage-driven concepts are useful for seeking coupling paths in a specific design, a myriad of potential coupling paths is expected for the wide range of approaches to design layout in applications as diverse as computer, automotive, avionic, and industrial electronics.

## Acknowledgements

The authors gratefully acknowledge the support of Allison Transmission for this project, as well as helpful discussions with Jerry Myerhoff and Sandy Walker of Motorola, and the EMC Design Group at Compaq Computer.

## References

- [1] J. L. Drewniak, T. H. Hubing, and T. P. Van Doren, “Investigation of fundamental mechanisms of common-mode radiation from printed circuit boards with attached cables,” *1994 IEEE Electromagnetic Compatibility Symposium Proceedings*, Chicago, IL, pp. 110-115, 1994.
- [2] A. E. Ruehli, “Inductance calculations in a complex integrated circuit environment,” *IBM J. Research and Development*, vol. 16, pp. 470-481, 1972.
- [3] C. R. Paul, “The concept of dominant effect in EMC,” *IEEE Trans. Electromagn. Compat.*, vol. 34, pp. 363-367, August 1992.
- [4] K. B. Hardin, J. T. Fessler, and D. R. Bush, “Spread spectrum clock generation for the reduction of radiated emissions,” *1994 IEEE Electromagnetic Compatibility Symposium Proceedings*, Chicago, IL, pp. 227-231, 1994.